Methane emissions offset atmospheric carbon dioxide uptake in coastal macroalgae, mixed vegetation and sediment ecosystems

Roth, Florian

2023-01

Article

Methane emissions offset atmospheric carbon dioxide uptake in coastal macroalgae, mixed vegetation and sediment ecosystems

Florian Roth [1,2] ✉, Elias Broman [1,3], Xiaole Sun [1,4], Stefano Bonaglia [5], Francisco Nascimento [1,3], John Prytherch[6], Volker Brüchert [7,8], Maysoon Lundevall Zara[7], Märta Brunberg[2], Marc C. Geibel [1], Christoph Humborg[1,2] & Alf Norkko[1,2]

Coastal ecosystems can efficiently remove carbon dioxide (CO_2) from the atmosphere and are thus promoted for nature-based climate change mitigation. Natural methane (CH_4) emissions from these ecosystems may counterbalance atmospheric CO_2 uptake. Still, knowledge of mechanisms sustaining such CH_4 emissions and their contribution to net radiative forcing remains scarce for globally prevalent macroalgae, mixed vegetation, and surrounding depositional sediment habitats. Here we show that these habitats emit CH_4 in the range of 0.1 – 2.9 mg CH_4 m^{-2} d^{-1} to the atmosphere, revealing in situ CH_4 emissions from macroalgae that were sustained by divergent methanogenic archaea in anoxic microsites. Over an annual cycle, CO_2-equivalent CH_4 emissions offset 28 and 35% of the carbon sink capacity attributed to atmospheric CO_2 uptake in the macroalgae and mixed vegetation habitats, respectively, and augment net CO_2 release of unvegetated sediments by 57%. Accounting for CH_4 alongside CO_2 sea-air fluxes and identifying the mechanisms controlling these emissions is crucial to constrain the potential of coastal ecosystems as net atmospheric carbon sinks and develop informed climate mitigation strategies.

Climate change mitigation demands reduced anthropogenic emissions of greenhouse gases (GHGs) and effective removal of excess carbon dioxide (CO_2) and methane (CH_4) from the atmosphere. Shallow-water coastal ecosystems can absorb and store large amounts of carbon from the atmosphere through vegetation buildup and long-term sediment burial[1]. This ecosystem function has raised worldwide interest in the scientific community, conservation organizations, and governmental bodies about the potential of these ecosystems in short-term climate mitigation[2–4]. In fact, restoring the carbon sequestration capacity of coastal ecosystems and improving their global management could result in an annual uptake of 841 (621–1064) Tg CO_2-equivalents (CO_2-eq.) per year, representing a significant GHG sink in the global carbon budget[4]. However, some of this organic carbon is metabolized and returned to the atmosphere as CH_4[5,6]. While aquatic CH_4 emissions can partly offset the GHG sink estimate of the terrestrial landscape[7] and of some vegetated coastal ecosystems, such as mangroves[8], the magnitude of CH_4 fluxes and their contribution to the net atmospheric GHG exchange remains unknown for the majority of

[1]Baltic Sea Centre, Stockholm University, Stockholm, Sweden. [2]Tvärminne Zoological Station, Faculty of Biological and Environmental Sciences, University of Helsinki, Hanko, Finland. [3]Department of Ecology, Environment and Plant Sciences, Stockholm University, Stockholm, Sweden. [4]Center of Deep Sea Research, Institute of Oceanology, Chinese Academy of Sciences, Qingdao, China. [5]Department of Marine Sciences, University of Gothenburg, Gothenburg, Sweden. [6]Department of Meteorology, Stockholm University, Stockholm, Sweden. [7]Department of Geological Sciences, Stockholm University, Stockholm, Sweden. [8]Bolin Centre for Climate Research, Stockholm University, Stockholm, Sweden. ✉e-mail: florian.roth@su.se

coastal environments and challenges our ability to develop informed climate mitigation strategies for these ecosystems[9].

Primary production from submerged and partially emerged coastal vegetation[10-12] and the associated accumulation of allochthonous carbon within or outside of these systems makes coastal environments some of the most carbon-rich ecosystems in the world[13-15]. While the high net ecosystem productivity is a main driver for the uptake of atmospheric CO_2 in vegetated ecosystems[16], the direct contribution to the sea-air CO_2 exchange remains understudied across many coastal environments[17]. In addition, methanogenic archaea in anoxic sediments associated with these ecosystems produce CH_4 during carbon burial, which adds to the release of locally fixed autochthonous and imported allochthonous carbon from these ecosystems[18,19]. To date, it is estimated that the coastal ocean contributes 5 – 28 Tg CH_4 yr^{-1} to total global CH_4 emissions[6,20]. Because CO_2 and CH_4 differ in their atmospheric lifetimes and radiative efficiencies – with CH_4 having a sustained-flux global warming potential (SGWP) 45 times more potent than CO_2 over a 100-year time horizon[21] – CH_4 emissions may substantially counterbalance the carbon sink capacity attributed to the local instantaneous atmospheric CO_2 uptake[22].

Yet, the majority of coastal ecosystem carbon assessments are still based on changes in sediment and biomass carbon inventories[23] or primary productivity measurements using oxygen[24] to infer GHG exchange with the atmosphere. These conventional methods assume that emissions to the atmosphere are in the form of CO_2, neglecting the part of the carbon pool that is metabolized to CH_4 with a higher radiative forcing. In addition, neither carbon burial nor benthic productivity necessarily leads to a direct net uptake of atmospheric CO_2 over the same surface area for which the carbon burial is considered. This is because, first, the water column separates the atmosphere from benthic systems and sea-air CO_2 gas exchange is also affected by lateral inorganic carbon inputs, buffer effects, and the residence time of CO_2 in the water column[16,25]. Second, buried sedimentary organic carbon is composed both of laterally imported allochthonous and locally produced autochthonous sources[26]. This implies that even if a system is net autotrophic and exhibits carbon burial, it may still function as a net source of atmospheric CO_2 locally if the remineralization of laterally imported carbon is high.

Simultaneous and continuous CO_2 and CH_4 sea–air flux measurements are, therefore, indispensable to determine whether a coastal ecosystem acts as a net source or sink of atmospheric carbon-based GHGs – that is, if it has a positive or negative effect on radiative forcing[21]. In situ automated cavity ring-down spectroscopy is particularly effective to quantify coastal sea-air CO_2 and CH_4 fluxes simultaneously – but its application has been limited to estuarine, mangrove, and seagrass systems[27-30]. The paucity of similar measurements across a wider range of coastal environments – for example, globally prevalent and highly productive macroalgae and mixed vegetation habitats, or their surrounding shallow depositional sediment areas – currently complicates efforts evaluating the realized potential of our coasts to remove carbon from the atmosphere. This is because (1) rigorous evidence for the uptake of atmospheric CO_2 by many such coastal systems through direct sea-air CO_2 gas exchange remains understudied[17], and (2) concurrent CH_4 emissions from these environments could offset or even negate their value as atmospheric carbon dioxide sinks[7].

In this study, we quantify hourly, daily, and seasonal sea-air CO_2 and CH_4 fluxes simultaneously using a fast-response automated gas equilibrator system for in situ continuous measurements across three globally prevalent shallow water (<4 m) coastal ecosystems to assess their direct contribution to sea-air GHG exchange. To represent systems with varying carbon dynamics, which are also underrepresented with regards to simultaneous and continuous CO_2 and CH_4 sea-air flux measurements, we quantify GHG fluxes in a northern temperate area of

the Baltic Sea in the following habitats: (a) 'macroalgae' (i.e., mainly *Fucus vesiculosus*) areas, which have a high primary production (and carbon sequestration) potential[31-34] but are usually not associated with CH_4 emissions due to the lack of sediments on rocky substrates; (b) areas with submerged 'mixed vegetation' (i.e., a mix of macrophytes and macroalgae) on soft sediments, which trap large amounts of allochthonous and autochthonous carbon; and (c) adjacent 'bare sediments' with marginal vegetation (<10% total vegetation, of which were mainly dislodged *F. vesiculosus*) that are common deposition sites with low primary productivity but a high potential of carbon remineralization. We complement in situ GHG measurements with sediment geochemistry and microbial community structure and diversity (16S rRNA gene sequencing) assessments to describe site-specific mechanism by which CH_4 emissions are sustained in these habitats.

Results and discussion

Dynamic CH_4 and CO_2 sea-air gas exchange across coastal ecosystems

High-resolution sea-air CH_4 flux measurements revealed that all habitats were net sources of CH_4 to the atmosphere during all study periods. There was high variability in the magnitude of these fluxes across habitats and seasons (Fig. 1a and Supplementary Table 1; statistics in Supplementary Table 2). We report in situ CH_4 sea-air fluxes in the order of 0.1 ± 0.0 to 1.8 ± 0.1 mg CH_4 m^{-2} d^{-1} (mean ± SE) from the macroalgae habitat. CH_4 emissions from macroalgae have previously only been reported from in vitro studies where macroalgae material was artificially fermented[35,36] or in situ from natural degradation of macroalgae (i.e., *Fucus vesiculosus*) on beaches as beach wrack[37]. Daily mean net CH_4 fluxes in the mixed vegetation and bare sediment areas ranged from 0.1 ± 0.0 to 2.9 ± 0.3 mg CH_4 m^{-2} d^{-1} and 0.1 ± 0.0 to 2.5 ± 0.2 mg CH_4 m^{-2} d^{-1}, respectively (Supplementary Table 1). The magnitude of these fluxes corroborates recent measurements in similar coastal environments with fluxes ranging from 0.6 to 8.3 mg CH_4 m^{-2} d^{-1} (ref. [38]). Across all habitats, CH_4 fluxes were one order of magnitude higher in summer and fall than in spring and winter (Supplementary Table 1). As methanogenesis exceeds CH_4 oxidation during warm periods[39,40], increased CH_4 production in summer and fall likely explains this observation. CH_4 emissions in summer and fall are also comparable to globally compiled values for other coastal vegetated systems, such as mangroves, salt marshes, and seagrass beds (i.e., median, range: 4.5, −1.1–1168.8; 3.6, −1.5–1509.8; and 1.0, 0.0–6.4 mg CH_4 m^{-2} d^{-1}, respectively)[5]. Over an annual cycle, the cumulative net fluxes of CH_4 to the atmosphere were 0.34 (±0.01) g CH_4 m^{-2} y^{-1} in the macroalgae, 0.55 (±0.03) g CH_4 m^{-2} y^{-1} in the mixed vegetation, and 0.38 (±0.02) g CH_4 m^{-2} y^{-1} in the surrounding bare sediment areas (data presented as cumulative annual net flux and propagated error using daily means and the associated uncertainty). Such spatial and temporal heterogeneity of CH_4 flux distribution in coastal ecosystems suggest that high-resolution measurements are urgently needed to improve the reliability of CH_4 estimates and confine the habitat-specific contribution to regional and global CH_4 budgets[40].

Daily mean net sea-air CO_2 fluxes ranged from -763 ± 99 mg CO_2 m^{-2} d^{-1} (mean ± SE; sink of atmospheric CO_2) to 390 ± 35 mg CO_2 m^{-2} d^{-1} (source of atmospheric CO_2), with significant differences across habitats and seasons (Supplementary Table 1; statistics in Supplementary Table 3). The macroalgae and mixed vegetation sites were net sinks of atmospheric CO_2 over diel cycles in spring, summer, and fall (Supplementary Table 1). The hourly fluxes displayed considerable temporal dynamics over diel cycles, with peak CO_2 uptake rates usually measured between 13:00–17:00 h (Fig. 1b) in the vegetated areas. The data confirms that sunlight stimulated photosynthetic activity of submerged vegetation, causing an undersaturation of $p$$CO_2$ in surface waters relative to the atmospheric equilibrium, and promoted direct
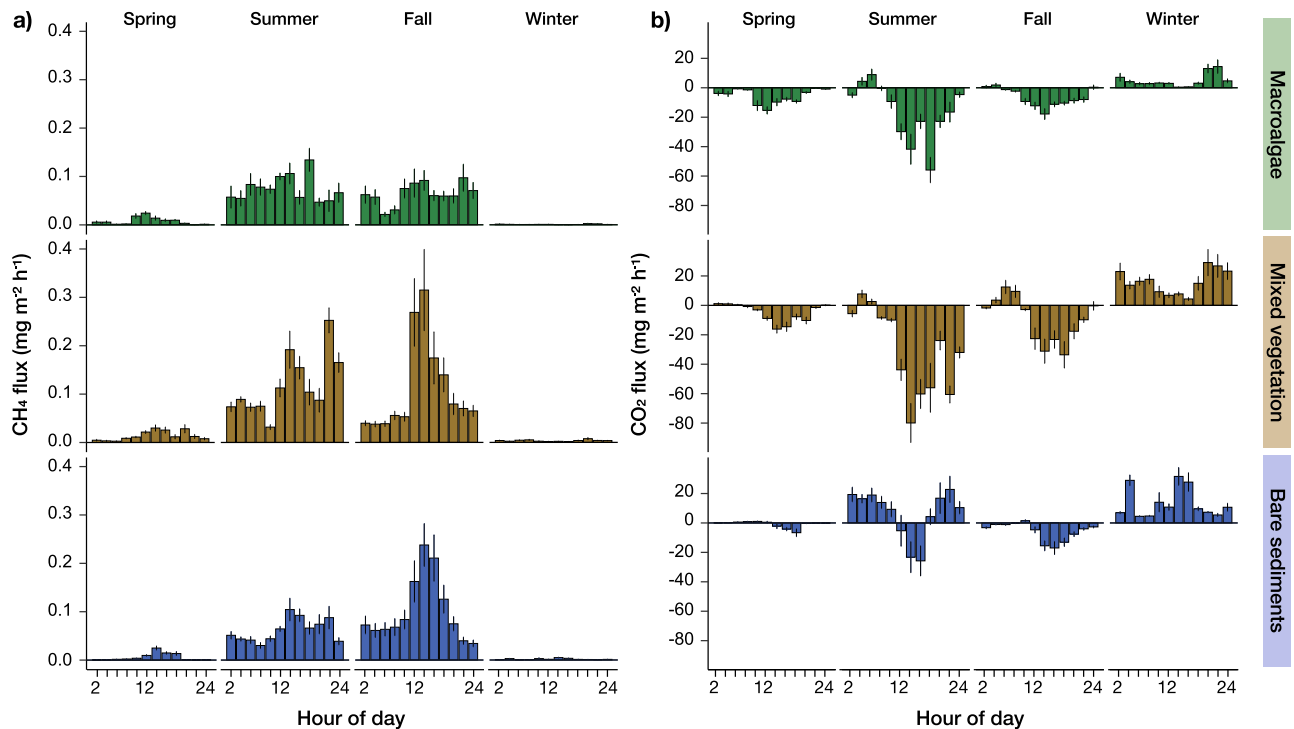
Fig. 1 | Hourly methane and carbon dioxide sea-air fluxes in coastal macroalgae, mixed vegetation, and bare sediment habitats. Hourly sea-air CH_4 (**a**) and CO_2 (**b**) fluxes across four seasons in three coastal ecosystems. Values are means ± standard error. Positive fluxes refer to an efflux from the water to the atmosphere (source), while negative fluxes depict an uptake of atmospheric GHGs (sink). In situ continuous (1 Hz) measurements were averaged to 15 min intervals and binned in 2-hour blocks for graphical representation. Daily integrated net sea-air fluxes of CH_4 and CO_2 across seasons and habitats are presented in the text and Supplementary Table 1.

net CO_2 removal from the atmosphere[16,41,42]. The surrounding bare sediment areas were moderate sinks of CO_2 in spring and fall (−21 ± 8 and −132 ± 17 mg CO_2 m^{-2} d^{-1}, respectively) compared to the vegetated habitats, and they became net sources of CO_2 in summer (157 ± 59 mg CO_2 m^{-2} d^{-1}). In photic sediments, ecosystem respiration can quickly outbalance or even outweigh CO_2 removal via photosynthesis, as photosynthetic activity remains limited to low-biomass microphytobenthos or dislodged macrophytes[32]. All habitats became net sources of atmospheric CO_2 over diel cycles in winter (Fig. 1b and Supplementary Table 1), suggesting a dominance of heterotrophic over autotrophic processes through suppressed photosynthetic activity in cold waters and insufficient light availability during this period of the year[32,43]. Over an annual cycle, the macroalgae and mixed vegetation habitats acted as net sinks of atmospheric CO_2 with cumulative fluxes of −52 (±5) and −71 (±10) g CO_2 m^{-2} y^{-1}, respectively (data presented as cumulative annual net flux and propagated error using daily means and the associated uncertainty). In comparison, the bare sediments were net sources of CO_2 to the atmosphere with 30 (±6) g CO_2 m^{-2} y^{-1}. The data confirm high rates of primary production across macrophyte and macroalgae canopies in similar geographic regions[31,32,44] and highlight that net ecosystem production in macroalgae beds and other submerged mixed vegetation can directly translate into atmospheric CO_2 removal[16,42,45].

CH_4 emissions offset the carbon sink capacity attributed to atmospheric CO_2 uptake

The simultaneous measurement approach of CH_4 and CO_2 sea-air fluxes is viable for directly comparing the direction and magnitude of carbon-based sea-air gas exchange and better constraining the net radiative balance of coastal habitats. We calculated the net sea-air GHG balance by converting CH_4 fluxes into CO_2-eq. fluxes based on the SGWP over a 100-year time horizon[21]. This measure describes metric-weighted GHG exchanges[22], i.e., the net CO_2-eq. flux is the sum of the CO_2-eq. fluxes of each gas (i.e., CO_2 and CH_4). The SGWP was chosen

since these coastal ecosystems continually exchange GHGs with the atmosphere, which is not captured by the one-time "pulse" emission basis of the global warming potential (GWP)[21]. In the following, the carbon sink capacity attributed to atmospheric CO_2 uptake refers to an instantaneous influx of CO_2 from the atmosphere into the water caused by undersaturation of pCO_2 in surface waters relative to the atmospheric equilibrium; note, this capacity does not relate to long-term carbon sequestration processes as burial or export.

We found that CO_2-eq. CH_4 fluxes substantially offset the carbon sink capacity attributed to the net atmospheric CO_2 uptake (Fig. 2a, b); however, the magnitude of this offset was variable across habitat types and seasons, depending on the magnitude of CO_2 relative to CO_2-eq. CH_4 fluxes (Fig. 2a). For example, some of the highest offset (i.e., 84%; Fig. 2 and Supplementary Table 1) was observed in the bare sediment habitats, where photosynthetic activity by microphytobenthos or dislodged macrophytes (leading to CO_2 uptake) is counterbalanced by ecosystem respiration (leading to CO_2 release)[32], and CH_4 fluxes are sustained by organic matter-rich soft sediments[46]. In contrast, highly productive macroalgae (leading to increased rates of CO_2 uptake) and marginal CH_4 emissions showed generally lower offsets in the carbon sink capacity attributed to atmospheric CO_2 uptake by concurrent CH_4 emissions. Seasonally, the greatest offsets by CO_2-eq. CH_4 fluxes were observed in summer and fall, reducing the net GHG balance by 21–44% in the macroalgae, 16–47% in the mixed vegetation, and 42–84% in the bare sediment habitats. In general, the offset was higher in fall due to the seasonal asynchronicity between CO_2 and CH_4 inventories (Fig. 2), which highlights the limitations of simple empirical functions, such as temperature relationships, for predicting ecosystem GHG fluxes[47]. Across all habitats, the contribution of CO_2-eq. CH_4 fluxes to the net GHG balance were marginal in winter (~1%), likely due to low CH_4 production at low temperatures[39]. Over an annual cycle, CO_2-eq. CH_4 fluxes lowered the net atmospheric CO_2-eq. sink capacity attributed to CO_2 uptake in the macroalgae habitats from −52 down to −38 g CO_2-eq. m^{-2} y^{-1} (i.e., 28% reduction) and from −71 down to −46 g CO_2-eq. m^{-2}
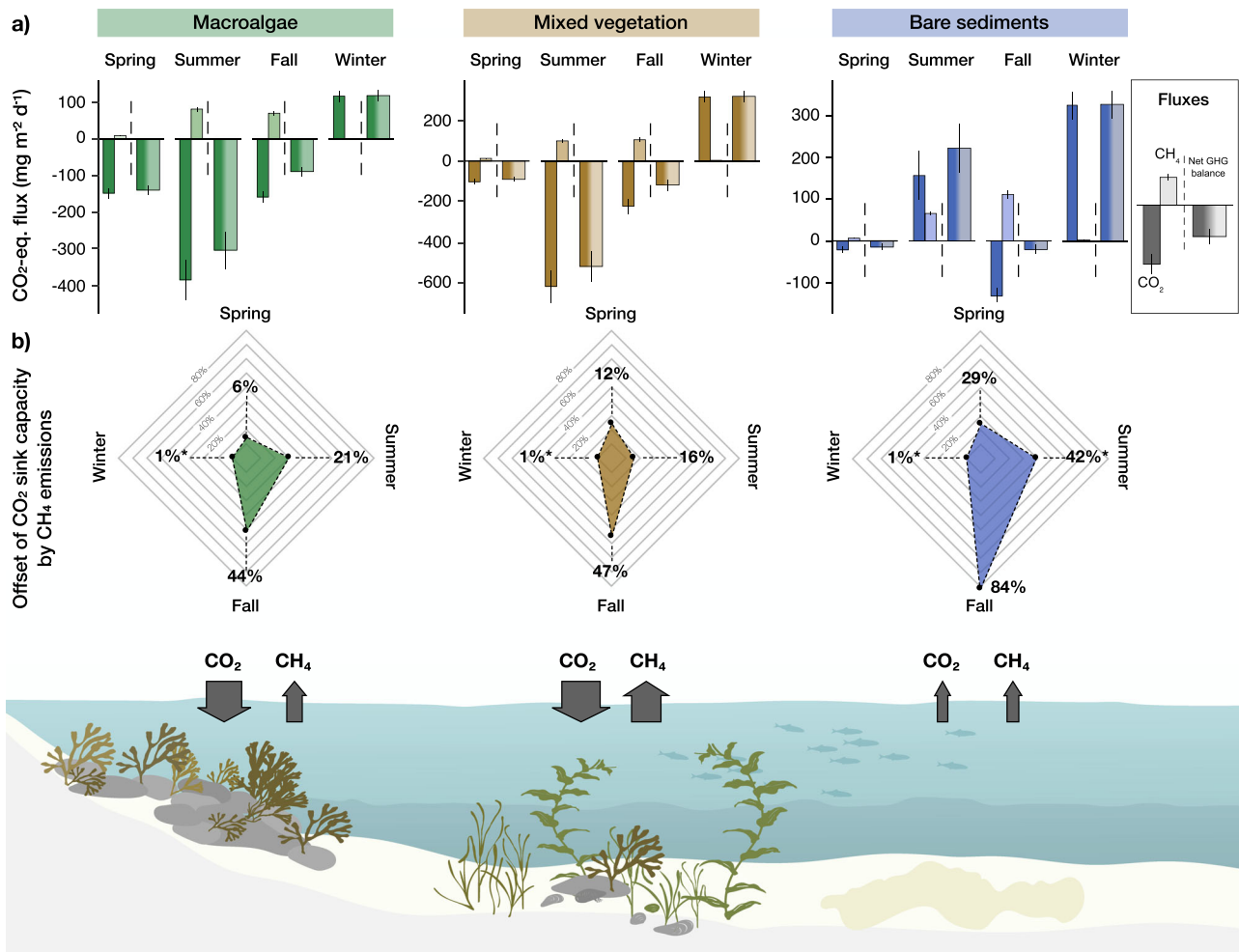
Fig. 2 | Seasonal net greenhouse gas balances. Daily mean net fluxes of CO_2, CH_4, and the net greenhouse gas balance (all expressed in CO_2-eq. fluxes) (**a**), and the offset (in %) of the carbon sink capacity attributed to atmospheric CO_2 uptake by CO_2-eq CH_4 emissions (**b**). Values in **a** are means ± standard error. Positive fluxes refer to an efflux from the water to the atmosphere (source), while negative fluxes depict an uptake of atmospheric GHGs (sink). CO_2-equivalent CH_4 fluxes were calculated using the sustained-flux global warming potential (SGWP) on a 100-year time horizon of 45[21]. The net greenhouse gas balance is calculated based on net CO_2 and net CO_2-eq. CH_4 fluxes. The offset in (b) is calculated from the net CO_2 flux and

the net CO_2-eq. CH_4 flux. An offset implies that the carbon sink capacity attributed to atmospheric CO_2 uptake was counterbalanced by concomitant CO_2-eq. CH_4 fluxes; an offset denoted with asterisk (*) implies that CO_2 emissions to the atmosphere were increased by the CO_2-eq. CH_4 flux. Note the different scales on the y-axis. Arrows at the water interface are conceptual and depict prevailing flux direction and magnitude in each habitat. Data for the daily net sea-air fluxes of CO_2, CH_4, CO_2-eq. of CH_4, and the net greenhouse gas (GHG) across four seasons in three coastal ecosystems are presented in Supplementary Table 1. Abbreviations: GHG = greenhouse gas. Original artwork by Elsa Wikander at Azote AB.

y^{-1} (i.e., 35% reduction) in the mixed vegetation habitats. Cumulative CO_2-eq. CH_4 fluxes augmented the positive net sea-air CO_2 fluxes of bare sediments by 57% (i.e., from 30 to 47 g CO_2-eq. m^{-2} y^{-1}).

Offsets in the coastal carbon sink capacity attributed to atmospheric CO_2 uptake by concurrent CH_4 emissions remain uncertain and difficult to compare because of the limited assessments in a few coastal ecosystems, such as mangroves[8] and seagrasses[48–50]. Our results show that CH_4 emissions from globally prevalent coastal habitats with unvegetated sediments, but also with productive macroalgae and mixed vegetation can lower the GHG sink estimate attributed to the atmospheric CO_2 uptake by one-third over an annual cycle. Thus, accounting for CH_4 alongside CO_2 sea-air fluxes becomes indispensable to correctly quantify the potential of coastal ecosystems to act as net atmospheric carbon sinks, which is necessary to develop informed climate mitigation strategies.

Distinct microbial communities shape habitat-specific CH_4 dynamics

High rates of CH_4 emissions have been ascribed to habitats with mixed vegetation[38,51] and surrounding depositional[52,53] areas with organic

matter-rich soft sediments. In general, these and similar coastal sediment systems account for the majority of total marine CH_4 emissions[20]. Rapid organic matter and sediment accumulation rates, deep anoxic sediment layers, bottom water oxygen depletion, and shallow sulfate-methane transition zones acting as "CH_4-filter" can all contribute to increased CH_4 release rates from coastal sediments[15,46,54]. The high rates of CH_4 emissions from the macroalgae habitats in our study are therefore intriguing because of the prevalence on rocky hard-bottom substrates and the absence of the above-mentioned "classical" sedimentary conditions that promote CH_4 formation. To examine whether the high surface water CH_4 concentrations (Supplementary Table 4) in the macroalgae habitat were a consequence of lateral transport of dissolved CH_4 from neighboring habitats or a unique feature of this particular location, we performed three additional assessments:

First, we sampled bottom substrates of all habitats across seasons to evaluate the local geochemical and microbial potential for CH_4 production. We found organic matter-rich anoxic sediments, with similar organic carbon contents (3–5%) below 10 cm depth in all habitats and months (Supplementary Fig. 1; selected results from summer are shown in Fig. 3a). While macroalgae grew on rocks,
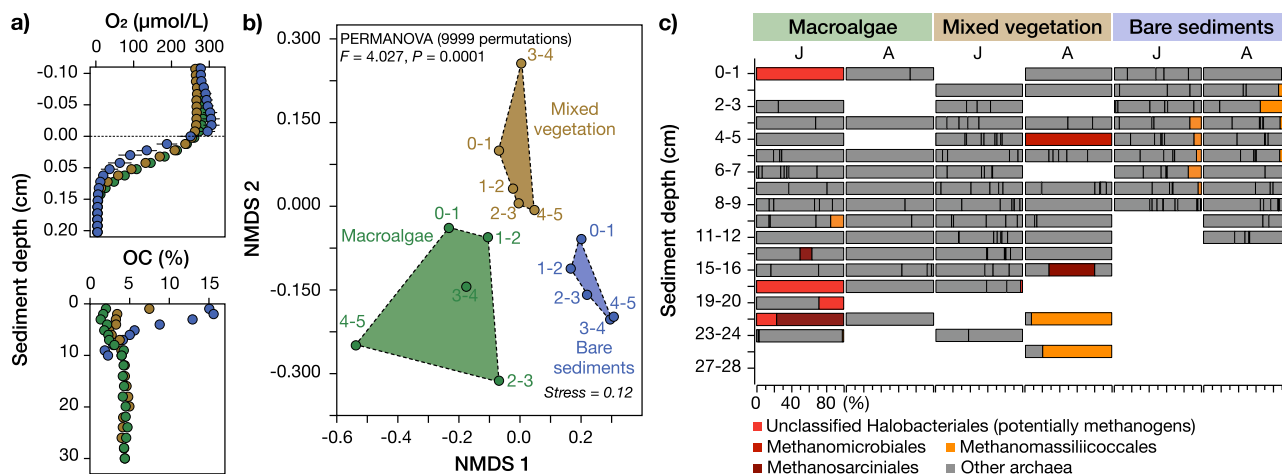
Fig. 3 | Habitat-specific sediment biogeochemical and microbial characteristics. Sediment biogeochemical (**a**) and microbial (**b**, **c**) characteristics during the sampling in summer. (**a**) Sediment microprofiles for O_2 and organic carbon (OC) contents. (**b**) NMDS plot of the Bray-Curtis dissimilarity index between the three habitats. The results are based on the whole 16S rRNA gene identified microbial community. The plot shows data from the first 5 cm layers in the sediment. The *pseudo-F* and *P* values show the statistical results from PERMANOVA (9999 permutations) based on testing all three habitats together. **c** Stacked bars showing the known methanogenic archaeal community (according to the SILVA v138.1 database) on the lowest taxonomic classified level during the sampling in July (J) and August (A). The y-axis shows the different sediment layers, while the x-axes show the relative abundance (% of all archaea, labels only shown on first x-axis). "Other archaea" denote groups <0.1% average of all samples. Taxonomic labels in color denote known methanogens in the dataset according to scientific literature. Note that for the station "bare sediments", samples could only be collected down to 9 cm (July) and 12 cm (August). Empty cells denote that no archaea were detected in the dataset.

organic matter-rich sediment was present in sediment pockets underlying the canopy, between rocks and boulders (exemplary picture in Supplementary Fig. 2a). Local organic carbon-rich deposits with anoxic conditions may be conducive to methanogenesis[13]. The presence of methanogens in these sediments was confirmed with 16S rRNA gene amplicon sequencing. However, the three habitats showed distinctively different microbial community structures in the top 5 cm of the sediment during all four seasons (Bray-Curtis dissimilarity analyses, PERMANOVA, $P = 0.0001$; Supplementary Figs. 3 and 4; example results from summer are shown in Fig. 3b), and methanogenetic archaea were detected at all sites (Fig S5; exemplifying results from summer shown in Fig. 3c). Some of the retrieved 16S rRNA gene sequences in the mixed vegetation and macroalgae systems were affiliated with classical methanogenic orders such as Methanomicrobiales (i.e., using hydrogen to produce CH_4) and methylotrophic Methanosarcinales (i.e., using one-carbon compounds such as methanol) (Supplementary Fig. 5; selected results from summer are shown in Fig. 3c)[55]. We also found unclassified sequences within the archaeal phylum Crenarchaeota (including the class Bathyarchaeia) in the macroalgae habitat (Supplementary Fig. 5). Some of these archaea encode the universal phylogenetic marker gene *mcrA* used to identify methanogenic microorganisms[56]. The bare sediments showed a prevalence of methylotrophic methanogens of the order Methanomassiliicoccales near the sediment surface (Supplementary Fig. 5; results from summer shown in Fig. 3b), which are major CH_4 producers in mangroves systems[57]. Finally, deeper oxygen penetration depths (Supplementary Fig. 1) in the mixed vegetation habitat are consistent with a higher relative abundance of methane-oxidizing Methylococcales bacteria, suggesting a more efficient sedimentary CH_4 oxidation filter in this habitat compared to the macroalgae and bare sediment area (Supplementary Fig. 6). Together, the data show that distinct methanogenic communities in vegetated and unvegetated habitats are likely involved in producing CH_4 in sediments or sediment pockets between rocks locally[50].

Second, we took samples of organic matter aggregates (floating filamentous algal and/or organic matter debris) associated with dense stands of macroalgae (Supplementary Fig. 2a, b) to test whether there were potential non-sedimentary CH_4 sources. Anaerobic microsites in dense stands of submerged macrophytes have previously been shown to provide suitable substrate for methanogenic archaea and are a habitat for several aquatic microorganism that produce CH_4 via classic methanogenic pathways in an otherwise aerobic water column[58]. Indeed, 16 S rRNA gene amplicon sequencing of algal and/or organic matter debris in the macroalgae habitat confirmed the presence of methanogenic archaea classified as family Methanobacteriaceae, and genera *Methanocorpusculum*, *Methanomethylophilus*, and *Methanobrevibacter* (Supplementary Fig. 7). Together, these methanogens can use various substrates for methanogenesis, such as CO_2, acetate, and methylated compounds[59], suggesting a possible involvement of divergent CH_4 metabolisms within microsites of *Fucus vesiculosus* habitats that could act as sources of non-sedimentary CH_4 production. Importantly, methylotrophic methanogenesis can proceed in saline to hypersaline environments with high ambient sulfate concentrations[50,60,61] and is, thus, expected to also play an important role in coastal environments with higher salinity compared to the brackish waters of the Baltic Sea.

Lastly, we expanded our surface water CH_4 concentration measurements to a macroalgae-dominated area in the Gulf of Finland, 400 km east of our initial field site, to test whether: (1) measurements of high surface water CH_4 concentrations (Supplementary Table 4) in the macroalgae habitat of our main study area also occur at other locations; and (2) non-sedimentary CH_4 sources within coastal macroalgae habitats are sufficient to increase surface water CH_4 concentrations to a value above open water control observations. For this reason, measurements in the Finnish archipelago were performed in dense stands of *Fucus vesiculosus* that grew exclusively on hard bottom substrates surrounding a small rock island (Supplementary Fig. 8a). No sediment pockets underlying the macroalgae canopy were observed at this site. The results were compared to CH_4 concentrations measured in two open water control sites in 40–60 m distance to the island (Supplementary Fig. 8a). Results of a one-way ANOVA and subsequent Tukey's HSD Test for multiple comparisons (Supplementary Fig. 8b) found that the mean value of surface water CH_4 concentrations was significantly higher in the macroalgae site (mean = 56.69 nmol/L CH_4, SD = 0.76, $n = 70$) compared to the two open water locations (i.e., mean = 50.41 nmol/L CH_4, SD = 1.48, $n = 105$, $p < 0.0001$, 95% C.I. = [−6.95, −5.61]; and mean = 49.73 nmol/L CH_4, SD = 2.48, $n = 119$, $p < 0.0001$, 95% C.I. = [6.31, 7.62]). These results provide evidence for 1)

the occurrence of elevated surface water CH_4 concentrations across macroalgae habitats in various geographic locations and 2) local CH_4 production within macroalgae habitats even without underlying sediments.

While it becomes evident from the data that macroalgae habitats can produce and emit CH_4 locally – with possible sources from sediment pockets underlying the canopy, and/or anoxic organic matter microsites within dense stands that harbor methanogenic archaea – other indirect sources may also contribute to CH_4 formation in these oxic waters. For example, the production of CH_4 precursors and facilitation of their bacterial breakdown or chemical conversion have also been proposed[58] and warrant further investigations on the individual contribution of various sources and pathways of CH_4 production in macroalgae habitats.

Accounting for CH_4 emissions from a wide range of coastal environments is crucial to inform efforts addressing climate change mitigation

Identifying the locations and mechanisms responsible for changing global atmospheric CO_2 and CH_4 is still a critical challenge for predicting future interactions between the carbon cycle and climate. The role of vegetated coastal ecosystems as a climate mitigation tool has attracted attention worldwide, with many countries pledged to use such systems as part of their nationally determined GHG inventories. However, traditional views of the radiative balance of coastal ecosystems often fail to capture some of the complexity of how these systems can impact the climate. Specifically, despite growing evidence for widespread CH_4 emissions from coastal ecosystems[5,6], the contribution to the net atmospheric GHG exchange remains unknown for many such environments and creates challenges for developing informed climate mitigation strategies[9].

Here, we showed that CH_4 emissions have to be measured in conjunction with sea-air CO_2 exchange to comprehensively evaluate the direction and magnitude of carbon-based GHG exchange with the atmosphere[21] and evaluate the net radiative balance of globally important coastal ecosystem. While autotrophic fucoid seaweed and mixed vegetation communities assessed in this study may efficiently remove CO_2 from the atmosphere during most of the year (Fig. 1b), concurrent CH_4 emissions (Fig. 1a) offset up to one-third of the net carbon sink capacity attributed to atmospheric CO_2 uptake over an annual cycle (Fig. 2a, b). Interest in financing coastal restoration or afforestation through the sale of carbon offset credits[62] adds urgency to including counterbalancing CH_4 emissions to evaluate the atmospheric carbon removal function correctly. Notably, macroalgae habitats are proclaimed to be Earth's largest vegetated coastal biome with exceptionally high rates of net primary production[34], and are, thus, already part of such carbon offset schemes[63] but have no reported in situ CH_4 emission rates identified to date.

Therefore, we recommend including direct sea-air CH_4 alongside CO_2 flux measurements from a wider range of vegetated and unvegetated coastal environments in future assessments as a necessary step to: (1) improve baselines for tracking emission trends, which currently rely primarily on carbon stock changes[23] or productivity measurements using oxygen; (2) identify factors and processes that increase GHG emissions from coastal environments, as, for example, CH_4 emissions are highly sensitive to temperature[39] and anthropogenic perturbations[6]; (3) integrate long-term continuous observations with process-based biogeochemical models to reduce uncertainties in estimating coastal carbon budgets as well as their climate effects; and (4) appreciate the high spatiotemporal heterogeneity in vegetation cover and functions related to carbon turnover of coastal ecosystems, which presently challenges GHG flux estimates[9,40].

In conclusion, our simultaneous high-resolution sea-air CO_2 and CH_4 flux measurements show that CH_4 emissions can offset one-third of the carbon sink capacity attributed to atmospheric CO_2 uptake over an annual cycle across highly productive macroalgae and mixed vegetation coastal ecosystems in a northern temperate region. Net atmospheric CO_2 uptake still outweighs CO_2-eq. CH_4 emissions – that is, these habitats exert a net cooling impact over centurial timescales. This net radiative forcing benefit contrasts surrounding unvegetated sediment areas, which act as net atmospheric CO_2 and CH_4 source. Thus, the conservation and restoration of vegetated coastal ecosystems is advocated because it may effectively remove CO_2 from the atmosphere and reduce the adverse effects of climate change. However, the coastal atmospheric carbon sink capacity may be smaller than currently established, as spatially and temporally resolved CH_4 emissions remain unaccounted for in many coastal environments. Knowledge on habitat-specific CH_4 production pathways[50], including potential oxic CH_4 production mechanisms[58], and data on CH_4 emissions from various coastal ecosystems are, thus, needed to inform efforts addressing climate change with the net potential of coastal ecosystems to act as atmospheric carbon sinks.

Methods
Study area
The study was conducted on the island of Askö in the Baltic Sea (58°49′15.4″N 17°38′08.8″E) in 2020. Three distinct shallow (<4 m water depth) coastal habitats were identified according to their dominant type of substrate and vegetation: (1) Mixed-vegetated communities of vascular plants and algae on sediments (hereafter 'mixed vegetation' habitat; (2) macroalgae on rocks with pockets of sediments (hereafter 'macroalgae' habitat), and (3) surrounding soft sediments with marginal macrovegetation cover (hereafter 'bare sediments'). Each habitat was assessed visually, and the percent cover of the underlying substrate and macrovegetation was recorded within a 5 m radius. Benthic surveys were repeated in April and September 2020. The habitat with 'mixed vegetation' was characterized by coarse sediments with 60–90% total vegetation cover. The vegetation was dominated in equal parts by vascular plants (e.g., *Phragmites australis*, *Stuckenia pectinata*, and *Ruppia spiralis*) and benthic algae (e.g., *Chara aspera* and heterogenous assemblages of filamentous algae). The 'macroalgae' habitat was situated on rocks and boulders with pockets of permeable sediments with 80–95% total vegetation cover comprised of the macroalgae *Fucus vesiculosus*, and *Ulva* spp., the encrusting *Hildenbrandia rubra*, and various filamentous algae. No vascular plants were identified in this habitat. The surrounding 'bare sediment' habitat had 7–10% total vegetation, of which were mainly dislodged *F. vesiculosus* and filamentous algae. The habitats were fully submerged at all times due to the absence of tides in this region of the Baltic Sea[64]. The average of measured salinities in the studied habitats ranged from 6.6 to 7.0 over the course of the year, and, thus, reflected brackish water conditions typical for the central Baltic Sea with freshwater inflows from land and limited salt water inflows from the Danish straits. However, locally at the study site on the island in the outer Stockholm archipelago, there were no major freshwater inputs from rivers or streams, which is reflected by relatively constant salinity throughout the measurement period. Additional assessments were conducted in the Finnish archipelago in the Baltic Sea (59°50′30.8″N 23°15′01.0″E) in October 2021. Details about this site and the measurements performed are outlined in the section "CH_4 concentration measurements within and outside of a macroalgae-dominated habitat of the Finnish archipelago".

Quantification of surface water and atmospheric CO_2 and CH_4
The partial pressures of surface water and atmospheric CO_2 and CH_4 in the three habitats were quantified during four measurement periods over an annual cycle (i.e., spring = 18–29 May; summer = 06–11 July; fall = 22 October to 2 November; and winter = 30 November to 08 December 2020). CO_2 and CH_4 concentrations were measured using a

fast-response automated gas equilibrator and cavity ring-down spectrometer (CRDS; model G2201-i, Picarro Inc.) according to protocols outlined in Roth et al. (2022)[40]. Briefly, surface water (at around 30 cm depth) was drawn in by a submersible pump from a floating ponton that was positioned over the habitats, and the water was transferred to a showerhead equilibrator (1 L headspace volume). From the equilibrator, a continuous air loop was linked to the CRDS, where CO_2 and CH_4 were measured in the dried gas stream for 35 minutes, followed by gas measurements of ambient air for 10 minutes (i.e., one complete cycle was 45 minutes). These measurement cycles ran continuously during the measurement periods mentioned above and the ponton with the submersible pump was moved between the defined habitats every 24 h. Concentrations measured at 1 Hz frequency were averaged and logged every 10 s. The recorded data were filtered by removing data from the transition period between stations and ambient air and water measurements due to the response time of CRDS to sharp changes in concentrations. Data was also removed during improper functioning (e.g., low water flow).

Environmental data

Alongside CRDS measurements, several environmental and meteorological variables were recorded. Before the showerhead equilibrator, surface water was pumped into a flow-through chamber, where ancillary data (salinity, temperature) were measured with every CRDS measurement using a thermosalinograph (Seabird TSG 45). Surface water temperature, pH, and dissolved oxygen concentrations at the point of water intake were logged every 15 min using a multiparameter sonde (model EXO2, YSI) that was calibrated prior to each deployment. Wind data observations (wind speed and direction) and air temperature were obtained from a Metek uSonic-3 heated 3D sonic anemometer, and a Vaisala HMP155 shielded temperature probe mounted on a 1.5 m high meteorological mast. The mast was located at the waterline, ~400 m to the northwest of the sampled habitats. Mean winds were adjusted to a 10 m reference height assuming a logarithmic profile with neutral stability:[65]

$$U_{10} = U + \left(\frac{u^*}{kappa}\right) \times \log(\frac{10}{zu}) \tag{1}$$

where U is the measured wind speed at height zu, u^* is the measured friction velocity by the 3D sonic anemometer, and kappa is the von Karman constant (0.4). Environmental data as well as surface water CO_2 and CH_4 concentrations are presented in Supplementary Table 4.

Sea-air flux computation of CO_2 and CH_4

The sea-air flux (F) of CO_2 or CH_4 is calculated as:

$$F = k \times K_0 \times (pGas_{sea} - pGas_{air}) \tag{2}$$

where k (m s^{-1}) is the gas transfer velocity, K_0 (mol m^{-3} atm^{-1}) is the aqueous-phase solubility of the respective gas, and $pGas_{sea}$ and $pGas_{air}$ are the measured partial pressures of CO_2 or CH_4 in the near-surface water and in the air, respectively. The solubilities were determined from Weiss 1974[66] for CO_2 and Wiesenburg and Guinasso 1979[67] for CH_4 as:

$$\ln \beta = A1 + A2\left(\frac{100}{T}\right) + A3\ln\left(\frac{T}{100}\right) + S\left[(B1 + B2(T/100) + B3(T/100)^2\right] \tag{3}$$

where β is the dimensionless (mL of gas dissolved per mL of H_2O) Bunsen solubility coefficient, A1, A2, A3, and B1, B2, and B3 are constants, T is the measured water temperature (K) and S the measured salinity. Assuming CH_4 behaves as an ideal gas, K_0 is related to β in the above formula by $K_0 = \beta (R \times T_{STD})^{-1}$, where R (m^3 atm K^{-1} mol^{-1}) is the ideal gas constant and T_{STD} (K) is the standard temperature in Kelvin.

The gas transfer velocity (k) used is that determined by Wanninkhof[68], as:

$$k = 0.251 \times U^2 \times \left(\frac{Sc_{balticsea}}{660}\right)^{-0.5} \tag{4}$$

where U is the wind speed (m s^{-1}) at 10 m height and $Sc_{balticsea}$ is the Schmidt number at the measurement site, which is dependent on temperature, salinity, and gas molecule. Sc was corrected for the corresponding temperature that was measured simultaneously with partial pressures the gases according to coefficients taken from Wanninkhof[68]. Further, the Schmidt number for Baltic Sea brackish water (i.e., $Sc_{balticsea}$) with measured salinity ($S_{balticsea}$) was calculated by interpolation of Sc for fresh water (salinity 0‰) and seawater (salinity 35‰) following refs. 69 and [70]:

$$Sc_{balticsea} = \frac{(Sc_{seawater} - Sc_{freshwater}) \times S_{balticsea}}{35} \times Sc_{freshwater} \tag{5}$$

Other variables (e.g., currents, waves, water depth) can also be used to predict k in coastal environments, but the studied location does not have any significant permanent or tidal currents, and estuarine models may not provide better results for our setting. Further, Lundevall-Zara et al.[38] tested other wind-based k models in similar habitats of the same location and concluded that calculated average k-values from different models were close to those of the Wanninkhof[68] relationship for the range of wind velocities encountered on the island of Askö. Fluxes were expressed in mg m^{-2} day^{-1} using the molecular weights of 44.01 g/mol and 16.04 g/mol for CO_2 and CH_4, respectively. First order estimates of annual fluxes (expressed in g CO_2 m^{-2} y^{-1} and g CH_4 m^{-2} y^{-1}) are based on cumulative fluxes for each season.

We used the sustained-flux global warming potential (SGWP) as a greenhouse gas metric to describe the relative radiative impact of a standardized amount of gas over a defined time horizon[21]. Specifically, over a 100-year time horizon, the SGWP of CH_4 is 45 times greater than that of CO_2, on a mass basis, based on:

$$CO_2 - eq_{(CH_4)} = F_{(CH_4)} \times SGWP_{(CH_4)} \tag{6}$$

where the CO_2-equivalent flux of methane (CO_2-eq$_{(CH4)}$) is the product of the flux ($F_{(CH4)}$) of CH_4 and its SGWP (i.e., 45) over the time horizon of 100 years.

Sediment sampling

We collected multiple sediment cores for sediment biogeochemical and microbial assessments in May, July, August, and December 2020 (i.e., spring, summer, and winter; no sediment cores were taken in fall due to logistical constraints). In the mixed vegetation and macroalgae habitats, acrylic cores (50 cm length; 7 cm inner diameter) were pushed into the sediments by hand and the cores were subsequently plugged with rubber stoppers for transportation to the laboratory. While macroalgae grew on rocky substrates, we sampled sediment pockets underlying the canopy in-between rocks and boulders (exemplary picture in Supplementary Fig. 2a). Sediment was sampled using a Kajak core sampler with acrylic core liners (50 cm length; 7 cm inner diameter) for sampling in the bare sediment area. In total, we took three cores per habitat and sampling event, one each for O_2 microprofiles, sediment organic carbon contents, and DNA extraction.

Bottom water and sediment microprofiles for O_2 were performed with a 100-µm tip microsensor (OX-100, Unisense) that was maneuvered by a motor-driven micromanipulator (Unisense). Above the sediment, a water column layer of 4–6 cm was kept circulated by a gentle air flow to maintain a constant diffusive boundary layer during measurements. Signals were recorded and converted into concentrations with a four-channel multimeter (Unisense). Concentrations were

measured at a vertical resolution of 100 μm. Profiles were made in triplicates in each subsampled sediment core and were performed within few hours after sampling. The O_2 microsensor was calibrated using a two-point calibration procedure in O_2 saturated water conditions (100% O_2 air saturation) and inside the sediment (0% O_2 air saturation). We report oxygen penetration depth (OPD) as the depth where O_2 concentration became <1 μM[71].

One core from each habitat and sampling period was used for estimating sediment organic carbon contents. In the laboratory, the cores were sliced at 1 cm intervals in the first 10 cm, and in 2 cm intervals thereafter. Organic carbon content in 5 mL subsample from each slice was estimated as a gravimetric loss-on-ignition (LOI) after combustion at 550 °C for 12 h.

Sediment for DNA extraction were sampled from cores with pre-drilled holes at 1 cm intervals. One core was collected per habitat and time point, yielding a total of 193 samples. During sampling, the holes were covered with water resistant tape that was later lifted and a sterile 3 ml syringe (Henke-Ject) was inserted to sub-sample the sediment. The sediment was transferred to 15 ml centrifuge tubes (Sarstedt) and stored at −20 °C until DNA extraction.

Sediment DNA extraction, 16S rRNA gene amplification, and sequencing

DNA was extracted from 0.25 g thawed and homogenized sediment from each sample using the DNeasy PowerSoil Pro Kit (QIAGEN) following the manufacturer's instructions. In addition, two blanks (only containing lysis buffer solution CD1) were extracted for DNA following the manufacturer's instructions. DNA quantity and quality were measured on a NanoDrop one spectrophotometer (Thermo Scientific). The DNA was stored at −80 °C until shipped to Novogene (Cambridge, UK) for PCR amplification, library preparation, and sequencing. The DNA concentration was normalized by Novogene according to their in-house company protocols. Amplification of the 16S rRNA gene V4 region was conducted with the primers 515 F[72] and 806 R[73], and library preparation was conducted using the NEBNext® Ultra™ II DNA Library Prep Kit with index adapters synthesized in-house by Novogene. The library was sequenced on the Illumina NovaSeq 6000 SP platform with a 2 × 250 bp paired-end which yielded 18.9 million read-pairs. See Supplementary Data 1 for a full list of sample names, fastq file names, sequences obtained before and after quality trimming, number of amplicon sequence variants (ASVs) constructed etc. The raw sequencing data has been uploaded to NCBI GenBank (https://www.ncbi.nlm.nih.gov/bioproject/) and can be accessed at BioProject PRJNA756121.

Bioinformatics

The sequencing yielded on average of 97,077 read-pairs per sample (min: 30,288, max: 119,686). Illumina adapters were removed from the raw reads by using SeqPrep 1.2[74] with the parameters: -A AGATCGG AAGAGCACACGTCTGAACTCCAGTCA and -B AGATCGGAAGAGCGT CGTGTAGGGAAAGAGTGT. The sequences were then analyzed following the DADA2 pipeline[75] using the DADA2 1.21.0 package in R[76]. The following quality trimming parameters were used to remove primer sequences, low quality bases, and low quality reads: truncLen=c(240,240), maxEE=2, truncQ=2, maxN=0, rm.phix=TRUE, trimLeft=c(21, 22). The raw and filtered data were visualized as FastQC 0.11.9 reports using MultiQC 1.11[77,78] to ensure the filtering was successful. The error model was run using parameters: nread=1e6, MAX_CONSIST = 30; the merging step using minOverlap=10; and the chimera removal step using the parameters allowOneOff=TRUE and minFoldParentOverAbundance=4. The ASVs were annotated against the SILVA nr99 v138.1 database[79]. Singletons, chloroplasts, and mitochondria sequences were removed from the ASV table. Finally, ASVs only attributed to the blank samples and ASVs > 1000 counts in the blank samples were removed. The final dataset consisted of 18,717 ASVs and had on average 703 ASVs per sample (min: 162, max: 1155),

with an average of 51,837 read counts per sample (min: 16,453, max: 74,843). The data were analyzed as relative abundances (%) using the software Explicet 2.10.5[80]. The full list of the DADA2 results including ASVs with their partial 16S rRNA gene sequence, classified taxonomy, and read counts is available in Supplementary Data 1.

Analysis of filamentous floating algal and/or organic matter debris associated with dense stands of macroalgae

Floating filamentous algal and/or organic matter debris associated with dense stands of macroalgae (exemplary pictures in Supplementary Fig. 2a, b) were collected in the macroalgae habitats of the main sampling site (58°49′15.4″N 17°38′08.8″E) in August 2020. Three samples were collected in 50 ml centrifuge tubes and flash frozen in liquid nitrogen and stored at −80 °C. DNA was extracted from 3 g homogenized material using the DNeasy PowerWater kit (Qiagen). The DNA was then handled and sequenced as mentioned in the section "Sediment DNA extraction, 16S rRNA gene amplification, and sequencing", except that the archaeal 16S rRNA gene V4–V5 region was amplified by the Novogene sequencing facility using primers Arch519F (CAGCCGCCGCGGTAA) and Arch915R (GTGCTC CCCCGCCAATTCCT)[81]. The delivered sequencing data had already been pre-trimmed for primers by Novogene and was analyzed with DADA2 using quality trim settings maxEE=2, truncQ=2, maxN=0, truncLen=c(215,215); error model nbases=1e8; merging minOverlap=10, maxMismatch=0; and chimera removal removeBimeraDenovo(method = "consensus"). The data were annotated against the SILVA NR99 v138.1 database. The final ASV counts were normalized as relative abundances (%). The full list of the DADA2 results including ASVs with their partial 16S rRNA gene sequence, classified taxonomy, and read counts is available in Supplementary Data 1.

CH_4 concentration measurements within and outside of a macroalgae-dominated habitat of the Finnish archipelago

To test whether measurements of high surface water CH_4 concentrations (Supplementary Table 4) in the macroalgae habitat of our main study site could also be found in other shallow coastal locations dominated by macroalgae, we expanded CH_4 concentration measurements to a macroalgae-dominated area 400 km further east to our original field site. The measurements in the Finnish archipelago (59°50′ 30.8″N 23°15′01.0″E) were performed in an exposed, dense stand of *Fucus vesiculosus* that grew on hard bottom substrates without any apparent sediment pockets underlying the canopy. Specifically, we selected a rocky island and measured surface water CH_4 concentrations in the *Fucus vesiculosus* stands directly surrounding the island, and in "open water" control sites in 40 – 60 m distance to the island (Supplementary Fig. 8). Surface water CH_4 concentrations were measured according to the protocol outlined in the section "Quantification of surface water and atmospheric CO_2 and CH_4". Surface water CH_4 concentrations were recorded continuously for 1 h in each location (see Supplementary Fig. 8A: location "1" = within the dense macroalgae stands directly surrounding the island; "2" = open water control site; "3" = open water control site) between 09:00 – 12:00 on October 13, 2021. A one-way ANOVA with Tukey's HSD Test for multiple comparisons was performed to compare the effect of the three different locations on surface water CH_4 concentrations (results presented together with Supplementary Fig. 8).

Data analysis

GHG flux data did not fulfill the requirements for general linear models (normal distribution of the dependent variables within groups, homogeneity of variances); thus, we performed the align-and-rank data for nonparametric factorial ANOVA procedure according to Wobbrock et al.[82]. After data preparation according to Wobbrock et al.[82], we performed two-way repeated measures ANOVAs in order to determine whether there was a significant interaction between the two

within subject factor variables "habitat" (i.e., the three habitat types 'macroalgae', 'mixed vegetation', and 'bare sediments') and "season" (i.e., sampling time-point in 'spring', 'summer', 'fall', and 'winter') on the dependent variables (i.e., 'CO_2' and 'CH_4' flux data), considering the individual subject identifier (i.e., habitat ID).

The 16S rRNA gene ASV data (normalized as relative abundance %) was used to construct non-metric multidimensional scaling (NMDS) plots based on the Bray-Curtis dissimilarity index and PERMANOVA (9999) tests using the software Past 4.07b[83].

Data availability
All data needed to evaluate the conclusions in the paper are present in the paper and/or the Supplementary Materials. Source data for all CH_4, CO_2, and CO_2-eq. CH_4 fluxes (hourly and daily integrated), 16S rRNA gene ASV tables, and sediment organic carbon content and oxygen penetration profiles are provided with this paper. Raw sequencing data that support the findings of this study have been deposited in the NCBI GenBank (https://www.ncbi.nlm.nih.gov/bioproject/) with the accession code: BioProject PRJNA756121. Source data are provided with this paper.

References
1. Mcleod, E. et al. A blueprint for blue carbon: toward an improved understanding of the role of vegetated coastal habitats in sequestering CO 2. *Front. Ecol. Environ.* **9**, 552–560 (2011).
2. Macreadie, P. I. et al. The future of Blue Carbon science. *Nat. Commun.* **10**, 1–13 (2019).
3. Lovelock, C. E. & Duarte, C. M. Dimensions of Blue Carbon and emerging perspectives. *Biol. Lett.* **15**, 20180781 (2019).
4. Macreadie, P. I. et al. Blue carbon as a natural climate solution. *Nat Rev Earth Environ* **2**, 826–839 (2021).
5. Al-Haj, A. N. & Fulweiler, R. W. A synthesis of methane emissions from shallow vegetated coastal ecosystems. *Glob. Chang. Biol.* **26**, 2988–3005 (2020).
6. Rosentreter, J. A. et al. Half of global methane emissions come from highly variable aquatic ecosystem sources. *Nat. Geosci.* https://doi.org/10.1038/s41561-021-00715-2 (2021).
7. Bastviken, D., Tranvik, L. J., Downing, J. A., Crill, P. M. & Enrich-Prast, A. Freshwater methane emissions offset the continental carbon sink. *Science (80-)* **331**, 50–50 (2011).
8. Rosentreter, J. A., Maher, D. T., Erler, D. V., Murray, R. H. & Eyre, B. D. Methane emissions partially offset "blue carbon" burial in mangroves. *Sci. Adv.* **4**, eaao4985 (2018).
9. Rosentreter, J. A., Al-Haj, A. N., Fulweiler, R. W. & Williamson, P. Methane and nitrous oxide emissions complicate coastal blue carbon assessments. *Glob. Biogeochem. Cycles* **35**, e2020GB006858 (2021).
10. Duarte, C. M., Middelburg, J. J. & Caraco, N. Major role of marine vegetation on the oceanic carbon cycle. *Biogeosciences* **2**, 1–8 (2005).
11. Snelgrove, P. V. R. et al. Global carbon cycling on a heterogeneous seafloor. *Trends Ecol. Evol.* **33**, 96–105 (2018).
12. Ortega, A. et al. Important contribution of macroalgae to oceanic carbon sequestration. *Nat. Geosci.* **12**, 748–754 (2019).
13. Barnes, R. O. & Goldberg, E. D. Methane production and consumption in anoxic marine sediments. *Geology* **4**, 297 (1976).
14. Reeburgh, W. S. Rates of biogeochemical processes in anoxic sediments. *Annu. Rev. Earth Planet. Sci.* **11**, 269–298 (1983).
15. Wallenius, A. J., Dalcin Martins, P., Slomp, C. P. & Jetten, M. S. M. Anthropogenic and environmental constraints on the microbial methane cycle in coastal sediments. *Front. Microbiol.* **12**, 631621 (2021).
16. Tokoro, T. et al. Net uptake of atmospheric CO2 by coastal submerged aquatic vegetation. *Glob. Chang. Biol.* **20**, 1873–1884 (2014).
17. Gallagher, J. B., Shelamoff, V. & Layton, C. Seaweed ecosystems may not mitigate CO2 emissions. *ICES J. Mar. Sci.* https://doi.org/10.1093/icesjms/fsac011 (2022).
18. Oremland, R. S. & Taylor, B. F. Sulfate reduction and methanogenesis in marine sediments. *Geochim. Cosmochim. Acta* **42**, 209–214 (1978).
19. Egger, M., Riedinger, N., Mogollón, J. M. & Jørgensen, B. B. Global diffusive fluxes of methane in marine sediments. *Nat. Geosci.* **11**, 421–425 (2018).
20. Weber, T., Wiseman, N. A. & Kock, A. Global ocean methane emissions dominated by shallow coastal waters. *Nat. Commun.* **10**, 1–10 (2019).
21. Neubauer, S. C. & Megonigal, J. P. Moving beyond global warming potentials to quantify the climatic role of ecosystems. *Ecosystems* **18**, 1000–1013 (2015).
22. Neubauer, S. C. Global warming potential is not an ecosystem property. *Ecosystems* https://doi.org/10.1007/s10021-021-00631-x (2021).
23. Howard, J., Hoyt, S., Isensee, K., Telszewski, M. & Pidgeon, E. Coastal blue carbon: methods for assessing carbon stocks and emissions factors in mangroves, tidal salt marshes, and seagrasses. 1–181 (2014). https://unesdoc.unesco.org/ark:/48223/pf0000372868.
24. Berg, P., Huettel, M., Glud, R. N., Reimers, C. E. & Attard, K. M. Aquatic eddy covariance: the method and its contributions to defining oxygen and carbon fluxes in marine environments. *Ann. Rev. Mar. Sci.* **14**, 431–455 (2022).
25. Tokoro, T., Watanabe, K., Tada, K. & Kuwae, T. Air–water CO2 flux in shallow coastal waters: theory, methods, and empirical studies. in *Blue Carbon in Shallow Coastal Ecosystems* 153–184 (Springer Singapore, 2019).
26. Saintilan, N., Rogers, K., Mazumder, D. & Woodroffe, C. Allochthonous and autochthonous contributions to carbon accumulation and carbon store in southeastern Australian coastal wetlands. *Estuar. Coast. Shelf Sci.* **128**, 84–92 (2013).
27. Ollivier, Q. R., Maher, D. T., Pitfield, C. & Macreadie, P. I. Net drawdown of greenhouse gases (CO2, CH4 and N2O) by a temperate australian seagrass meadow. *Estuaries Coasts* https://doi.org/10.1007/s12237-022-01068-8 (2022).
28. Maher, D. T. et al. Novel use of cavity ring-down spectroscopy to investigate aquatic carbon cycling from microbial to ecosystem scales. *Environ. Sci. Technol.* **47**, 12938–12945 (2013).
29. Call, M. et al. Spatial and temporal variability of carbon dioxide and methane fluxes over semi-diurnal and spring–neap–spring timescales in a mangrove creek. *Geochim. Cosmochim. Acta* **150**, 211–225 (2015).
30. Maher, D. T., Cowley, K., Santos, I. R., Macklin, P. & Eyre, B. D. Methane and carbon dioxide dynamics in a subtropical estuary over a diel cycle: Insights from automated in situ radioactive and stable isotope measurements. *Mar. Chem.* **168**, 69–79 (2015).
31. Attard, K. M. et al. Seasonal metabolism and carbon export potential of a key coastal habitat: The perennial canopy-forming macroalga Fucus vesiculosus. *Limnol. Oceanogr.* **64**, 149–164 (2019).
32. Attard, K. M. et al. Seasonal ecosystem metabolism across shallow benthic habitats measured by aquatic eddy covariance. *Limnol. Oceanogr. Lett.* **4**, 79–86 (2019).
33. Trevathan-Tackett, S. M. et al. Comparison of marine macrophytes for their contributions to blue carbon sequestration. *Ecology* **96**, 3043–3057 (2015).
34. Pessarrodona, A. et al. Global seaweed productivity. *Sci. Adv.* **8**, eabn2465 (2022).
35. Machado, L., Magnusson, M., Paul, N. A., de Nys, R. & Tomkins, N. Effects of marine and freshwater macroalgae on in vitro total gas and methane production. *PLoS ONE* **9**, e85289 (2014).

36. Hansson, G. Methane production from marine, green macro-algae. *Resour. Conserv.* **8**, 185–194 (1983).

37. Björk, M., Rosenqvist, G., Gröndahl, F. & Bonaglia, S. Methane emissions from macrophyte beach wrack on Baltic seashores. *Ambio* **52**, 171–181 (2023).

38. Lundevall-Zara, M., Lundevall-Zara, E. & Brüchert, V. Sea-air exchange of methane in shallow inshore areas of the Baltic sea. *Front. Mar. Sci.* **8**, 1–20 (2021).

39. Yvon-Durocher, G. et al. Methane fluxes show consistent temperature dependence across microbial to ecosystem scales. *Nature* **507**, 488–491 (2014).

40. Roth, F. et al. High spatiotemporal variability of methane concentrations challenges estimates of emissions across vegetated coastal ecosystems. *Glob. Chang. Biol.* https://doi.org/10.1111/gcb.16177 (2022).

41. Koweek, D. A. et al. A year in the life of a central California kelp forest: physical and biological insights into biogeochemical variability. *Biogeosciences* **14**, 31–44 (2017).

42. Watanabe, K. et al. Macroalgal metabolism and lateral carbon flows can create significant carbon sinks. *Biogeosciences* **17**, 2425–2440 (2020).

43. Möller, P., Pihl, L. & Rosenberg, R. Benthic faunal energy flow and biological interaction in some shallow marine soft bottom habitats. *Mar. Ecol. Prog. Ser.* **27**, 109–121 (1985).

44. Frigstad, H. *et al. Blue Carbon – Climate Adaptation, CO2 Uptake And Sequestration Of Carbon In Nordic Blue Forests – Results From The Nordic Blue Carbon Project.* (Nordic Council of Ministers, 2021).

45. Ikawa, H. & Oechel, W. C. Temporal variations in air-sea CO 2 exchange near large kelp beds near San Diego, California. *J. Geophys. Res. Ocean.* **120**, 50–63 (2015).

46. Reeburgh, W. S. Oceanic methane biogeochemistry. *Chem. Rev.* **107**, 486–513 (2007).

47. Davidson, E. A. & Janssens, I. A. Temperature sensitivity of soil carbon decomposition and feedbacks to climate change. *Nature* **440**, 165–173 (2006).

48. Oreska, M. P. J. et al. The greenhouse gas offset potential from seagrass restoration. *Sci. Rep.* **10**, 1–15 (2020).

49. Asplund, M. E. et al. Methane emissions from nordic seagrass meadow sediments. *Front. Mar. Sci.* **8**, 811533 (2022).

50. Schorn, S., Ahmerkamp, S., Bullock, E., Weber, M. & Lott, C. Diverse methylotrophic methanogenic archaea cause high methane emissions from seagrass meadows. *Proc. Natl Acad. Sci. USA.* https://doi.org/10.1073/pnas.2106628119/-/DCSupplemental.Published (2022).

51. Koebsch, F., Glatzel, S. & Jurasinski, G. Vegetation controls methane emissions in a coastal brackish fen. *Wetl. Ecol. Manag.* **21**, 323–337 (2013).

52. Sansone, F. J. & Martens, C. S. Methane production from acetate and associated methane fluxes from anoxic coastal sediments. *Science (80-).* **211**, 707–709 (1981).

53. Egger, M. et al. Rapid sediment accumulation results in high methane effluxes from coastal sediments. *PLoS ONE* **11**, e0161609 (2016).

54. Hamdan, L. J. & Wickland, K. P. Methane emissions from oceans, coasts, and freshwater habitats: New perspectives and feedbacks on climate. *Limnol. Oceanogr.* **61**, S3–S12 (2016).

55. Cai, M. et al. Metatranscriptomics reveals different features of methanogenic archaea among global vegetated coastal ecosystems. *Sci. Total Environ.* **802**, 149848 (2022).

56. Evans, P. N. et al. Methane metabolism in the archaeal phylum Bathyarchaeota revealed by genome-centric metagenomics. *Science (80-).* **350**, 434–438 (2015).

57. Zhang, C.-J., Pan, J., Liu, Y., Duan, C.-H. & Li, M. Genomic and transcriptomic insights into methanogenesis potential of novel methanogens from mangrove sediments. *Microbiome* **8**, 94 (2020).

58. Hilt, S., Grossart, H., McGinnis, D. F. & Keppler, F. Potential role of submerged macrophytes for oxic methane production in aquatic ecosystems. *Limnol. Oceanogr.* https://doi.org/10.1002/lno.12095 (2022).

59. Söllinger, A. & Urich, T. Methylotrophic methanogens everywhere — physiology and ecology of novel players in global methane cycling. *Biochem. Soc. Trans.* **47**, 1895–1907 (2019).

60. Karl, D. M. et al. Aerobic production of methane in the sea. *Nat. Geosci.* **1**, 473–478 (2008).

61. McGenity, T. J. & Sorokin, D. Y. Handbook of Hydrocarbon and Lipid Microbiology. p. 665–680 (Springer, 2010).

62. Murray, B. C., Pendleton, L., Jenkins, W. A. & Sifleet, S. *Green Payments for Blue Carbon Economic Incentives for Protecting Threatened Coastal Habitats* (Nicholas Institute for Environmental Policy Solutions, 2011).

63. Kuwae, T., Watanabe, A., Yoshihara, S., Suehiro, F. & Sugimura, Y. Implementation of blue carbon offset crediting for seagrass meadows, macroalgal beds, and macroalgae farming in Japan. *Mar. Policy* **138**, 104996 (2022).

64. Medvedev, I. P., Rabinovich, A. B. & Kulikov, E. A. Tides in three enclosed basins: the Baltic, Black, and Caspian Seas. *Front. Mar. Sci.* **3**, 46 (2016).

65. Haugen, D. A. *Workshop on Micrometeorology* (American Meteorological Society, 1973).

66. Weiss, R. F. Carbon dioxide in water and seawater: the solubility of a non-ideal gas. *Mar. Chem.* **2**, 203–215 (1974).

67. Wiesenburg, D. A. & Guinasso, N. L. Equilibrium solubilities of methane, carbon monoxide, and hydrogen in water and sea water. *J. Chem. Eng. Data* **24**, 356–360 (1979).

68. Wanninkhof, R. Relationship between wind speed and gas exchange over the ocean revisited. *Limnol. Oceanogr. Methods* **12**, 351–362 (2014).

69. Gülzow, W. et al. One year of continuous measurements constraining methane emissions from the Baltic Sea to the atmosphere using a ship of opportunity. *Biogeosciences* **10**, 81–99 (2013).

70. Jähne, B. et al. On the parameters influencing air-water gas exchange. *J. Geophys. Res.* **92**, 1937 (1987).

71. Bonaglia, S. et al. Meiofauna improve oxygenation and accelerate sulfide removal in the seasonally hypoxic seabed. *Mar. Environ. Res.* **159**, 104968 (2020).

72. Parada, A. E., Needham, D. M. & Fuhrman, J. A. Every base matters: assessing small subunit rRNA primers for marine microbiomes with mock communities, time series and global field samples. *Environ. Microbiol.* **18**, 1403–1414 (2016).

73. Apprill, A., McNally, S., Parsons, R. & Weber, L. Minor revision to V4 region SSU rRNA 806R gene primer greatly increases detection of SAR11 bacterioplankton. *Aquat. Microb. Ecol.* **75**, 129–137 (2015).

74. St John, J. *SeqPrep*. https://github.com/jstjohn/SeqPrep (2011).

75. Callahan, B. J. et al. DADA2: high-resolution sample inference from Illumina amplicon data. *Nat. Methods* **13**, 581–583 (2016).

76. R Core Team. *R: A Language And Environment For Statistical Computing* (R Foundation for Statistical Computing, 2021).

77. Andrews, S. *FastQC: A Quality Control Tool For High Throughput Sequence Data* (2010).

78. Ewels, P., Magnusson, M., Lundin, S. & Käller, M. MultiQC: summarize analysis results for multiple tools and samples in a single report. *Bioinformatics* **32**, 3047–3048 (2016).

79. Quast, C. et al. The SILVA ribosomal RNA gene database project: improved data processing and web-based tools. *Nucleic Acids Res* **41**, D590–D596 (2012).

80. Robertson, C. E. et al. Explicet: graphical user interface software for metadata-driven management, analysis and visualization of microbiome data. *Bioinformatics* **29**, 3100–3101 (2013).

81. Coolen, M. J. L. et al. Evolution of the methane cycle in Ace Lake (Antarctica) during the Holocene: response of methanogens and

methanotrophs to environmental change. *Org. Geochem.* **35**, 1151–1167 (2004).

82. Wobbrock, J. O., Findlater, L., Gergle, D. & Higgins, J. J. The aligned rank transform for nonparametric factorial analyses using only anova procedures. in *Proceedings of the SIGCHI Conference on Human Factors in Computing Systems* 143–146 (ACM, 2011).

83. Hammer, Ø., Harper, D. & Ryan, P. PAST: paleontological statistics software package for education and data analysis. *Palaeontol. Electron.* **4**, 1–9 (2001).

Author contributions

F.R., C.H., and A.N. conceptualized the study; F.R., X.S., M.C.G., and C.H. developed GHG flux methodology; E.B. and F.N. developed microbial methodology; C.H., A.N., J.P., E.B., F.N., S.B., and V.B. provided resources and material; F.R., E.B., X.S., S.B., F.N., J.P., M.L.Z., and M.B. performed investigation; F.R., E.B., S.B., M.L.Z, C.H., and A.N. contributed to formal data analysis and data interpretation; F.R., E.B., C.H., and A.N. wrote the original draft; all authors reviewed and edited the manuscript.

Competing interests

The authors declare no competing interests.

Additional information

Supplementary information The online version contains supplementary material available at https://doi.org/10.1038/s41467-022-35673-9.

Correspondence and requests for materials should be addressed to Florian Roth.

Peer review information *Nature Communications* thanks Celso Hernandez and the other, anonymous, reviewer(s) for their contribution to the peer review of this work. Peer reviewer reports are available.

Reprints and permissions information is available at http://www.nature.com/reprints

Publisher's note Springer Nature remains neutral with regard to jurisdictional claims in published maps and institutional affiliations.